Heat-Triggered Conversion of Protofibrils into Mature Amyloid Fibrils of β_2-Microglobulin†

Kenji Sasahara,‡ Hisashi Yagi,‡ Hironobu Naiki,§ and Yuji Goto*,‡

Institute for Protein Research, Osaka University, and CREST, Japan Science and Technology Agency, Yamadaoka 3-2, Suita, Osaka 565-0871, Japan, and Faculty of Medical Sciences, University of Fukui, and CREST, Japan Science and Technology Agency, Eiheiji, Fukui 910-1193, Japan

Received November 21, 2006; Revised Manuscript Received January 19, 2007

ABSTRACT: Heat-triggered conversion of the salt-induced thin and flexible protofibrils into well-organized thick and straight mature amyloid fibrils was achieved with β_2-microglobulin, a protein responsible for dialysis-related amyloidosis. First, protofibrils that formed spontaneously at pH 2.5 in the presence of 0.5 M NaCl were aggregated by agitating the solution. Second, the aggregated protofibrils were heated in a cell of a differential scanning calorimeter (DSC). The DSC thermogram showed an exothermic transition with sigmoidal temperature dependence, resulting in a remarkably large decrease in the heat capacity of the solution. Third, on the basis of electron microscopy together with circular dichroism spectroscopy, seeding experiments, and a thioflavin T binding assay, the sigmoidal transition was found to represent the conversion of protofibrils into mature amyloid fibrils. Furthermore, DSC thermograms obtained at various heating rates revealed that the transition curve depends on the heating rate, implying that the effects of heat associated with the conversion to the mature fibrils are kinetically controlled, precluding an interpretation in terms of equilibrium thermodynamics. Taken together, these results highlight the importance of the change in heat capacity in addressing the biological significance of interactions between solvent water and amyloid fibrils and, moreover, in detecting the formation of amyloid fibrils.

Protein aggregates, particularly amyloid fibrils, have begun to receive marked attention, as evidence accumulates that they are associated with the etiology of diseases such as Alzheimer's disease (amyloid β peptide), transmissible spongiform encephalopathy (prion), and dialysis-related amyloidosis [β_2-microglobulin (β2-m)[1], where the proteins in parentheses are amyloid precursors (*1*−*3*). Regardless of the original conformational state of the precursor, all amyloid fibrils share a common core structure made of cross β-sheets (*4*−*6*). Despite the importance of these fibrils in various biological phenomena, a comprehensive understanding of the mechanism by which amyloid fibrils form remains elusive. A wide variety of non-disease-associated proteins and peptides also have been shown to be capable of self-assembling into amyloid-like fibrils under suitable conditions, suggesting that certain general principles govern fibrillation (*7*, *8*).

β2-m, which constitutes the light chain of major histocompatibility complex type I (*9*), is a major component of the amyloid deposits found in patients with dialysis-related amyloidosis (*10*). In vitro, β2-m at neutral pH has been shown to be stably folded and highly intransigent to assembly into amyloid fibrils, and it is assumed that a partial or more substantial unfolding is required for fibrillation to occur (*11*−*14*). Under acidic conditions at pH 2.5 where β2-m is acid-unfolded, fibrillar structures are formed by at least two parallel routes depending on the ionic strength of the solution (*15*−*18*). In the presence of ∼0.2 M NaCl, well-organized mature fibrils with a needlelike morphology typical of amyloid fibrils that accumulated in patients' tissues are formed via a nucleation−growth mechanism involving a lag time. In this case, the addition of seed fibrils to the monomeric precursors effectively bypasses the nucleation step, leading to a rapid growth without a lag time (*11*). By contrast, at high concentrations of salt (∼0.5 M NaCl), β2-m does not form typical amyloid fibrils. Instead, it forms spontaneously thinner and more flexible fibrillar structures called protofibrils or protofilaments (*15*). No transformation from the salt-induced protofibrils into mature fibrils was observed in previous studies, so these two fibrillar structures are considered to form via distinct and competitive pathways (*15*, *17*, *18*). A unique feature of the salt-induced protofibrils is that their formation does not require the nucleation step characterized by a lag time. The salt-induced protofibrils and mature fibrils have distinct far-UV CD spectra of β-sheet structures that are centered around 212 and 219 nm, respectively (*15*). Furthermore, the salt-induced protofibrils exhibit less propensity to bind thioflavin T (ThT), a dye that specifically binds to organized β-sheet aggregates (*19*), suggesting relatively heterogeneous intermolecular interac-

† This work was supported by the Takeda Science Foundation and by Grants-in-Aid for Priority Areas (15076206) from the Japanese Ministry of Education, Culture, Sports, Science and Technology.

* To whom correspondence should be addressed: Institute for Protein Research, Osaka University, Yamadaoka 3-2, Suita, Osaka 565-0871, Japan. Telephone: 81-6-6879-8614. Fax: 81-6-6879-8616. E-mail: ygoto@protein.osaka-u.ac.jp.

‡ Osaka University.

§ University of Fukui.

[1] Abbreviations: β2-m, β_2-microglobulin; DSC, differential scanning calorimeter; CD, circular dichroism; $C_{p,app}$, apparent heat capacity; ThT, thioflavin T.

10.1021/bi602403v CCC: $37.00
Published on Web 02/23/2007

tions (*16*). However, the molecular mechanisms leading to distinct fibrillar structures are not well understood (*18*).

The aggregation of proteins is often triggered by a conformational alteration caused by temperature, pH, a chemical denaturant, etc. (*20*). Heat is a well-established stress factor that can lead to protein aggregation (*21*−*24*). However, the conformational and energetic aspects of heat-induced aggregation, particularly amyloid fibrillation, remain largely unclear (*13*). In two recent studies (*25*, *26*), we have shown the unique thermal response of mature amyloid fibrils of β2-m revealing kinetics featured with a characteristic heating rate dependence. This finding prompted us to extend our exploration of kinetic heat effects to fibrillation. In this study, when the effects of heat on the salt-induced protofibrils of β2-m were examined in detail, it was found that mature amyloid fibrils formed under certain conditions, in which a characteristic decrease in heat capacity with the kinetic feature accompanied the conversion. Our results suggest that the kinetic heat effect monitored by measuring the heat capacity of the protein solution is useful for sensitively detecting the formation of amyloid fibrils.

MATERIALS AND METHODS

Salt-Induced Fibrils. Recombinant human β2-m was expressed in *Escherichia coli* and purified according to procedures described previously (*27*). Salt-induced protofibrils of β2-m at 20−50 μM were formed by incubation for 24 h at 37 °C in 50 mM sodium citrate (pH 2.5) containing 0.5 M NaCl (*15*). Aggregation of the salt-induced protofibrils was performed using an isothermal titration calorimeter via agitation with the cylinder attached for 24 h at 37 °C (VP-ITC, Microcal, Northampton, MA). The rate of stirring was 310 rpm. Protein concentrations were determined spectrophotometrically at 280 nm using an extinction coefficient of 1.63 mL mg^{-1} cm^{-1} (*27*).

Calorimetric Measurements. DSC measurements were taken using a Microcal VP-DSC calorimeter, as described previously (*25*, *26*). Samples and buffers were carefully degassed by being stirred under vacuum before being loaded into the DSC sample and reference cells. Several heating−cooling−reheating cycles with the samples were performed in the temperature range of 10−100 (or 120) °C. After the buffer−buffer baseline was subtracted from the sample data, the apparent heat capacity ($C_{p,app}$) corresponding to the whole sample solution was evaluated using Origin (Microcal Inc.).

CD Measurements. CD spectra were recorded on an AVIV model 205s spectropolarimeter with a step size of 1 nm and an average time of 30 s using a quartz cell with a light path of 1 mm. The temperature of the sample solutions was maintained at 20 ± 0.1 °C by a thermoelectrically controlled cell holder attached to the polarimeter.

Transmission Electron Microscopy. The sample solution containing 30 μM β2-m was diluted 10-fold with pure water. Then, an aliquot (5 μL) of the diluted solution was placed on a copper grid (400-mesh) covered by a carbon-coated collodion film for 1 min, and the excess sample solution was removed by blotting with filter paper. The sample was negatively stained with a 2% (w/v) uranyl acetate solution for 1 min. Again, the liquid on the grid was removed by blotting with filter paper and dried. Electron micrographs were acquired using a JEOL 100CX transmission microscope with an acceleration voltage of 80 kV. The magnification was 29000×.

Light Scattering and ThT Fluorescence Measurements. Light scattering and ThT fluorescence were monitored with a Hitachi F-4500 spectrofluorometer using a quartz cell with a light path of 5 mm. For light scattering, the wavelengths for excitation and emission were both set at 350 nm. For ThT fluorescence, the intensity at 485 nm with an excitation wavelength of 445 nm was monitored. The temperature of the sample solutions was maintained at 25 ± 0.1 °C by a thermoelectrically controlled cell holder.

Seeding Reactions. Acid-unfolded β2-m at 30 μM in 50 mM sodium citrate at pH 2.5 and 100 mM NaCl was incubated at 37 °C with the seed fibrils at a final concentration of 5 μg/mL (0.42 μM). Aliquots of the sample were withdrawn at various intervals, and the light scattering intensity was measured at 25 °C with a Hitachi F-4500 spectrofluorometer.

RESULTS

Heat-Triggered Conversion of Salt-Induced Protofibrils into a Different Species. The light scattering intensity indicated that the formation of protofibrils at pH 2.5 was promoted by the increase in the NaCl concentration (Figure 1a), consistent with a previous study (*15*). At 0.5 M NaCl, the protofibrils exhibited a CD spectrum with a minimum at ∼212 nm (see Figure 3a below) (*15*). DSC thermograms of the protofibrils formed at 0.5 M NaCl exhibited a small endothermic (i.e., positive) peak centered at 85 °C, followed by an exothermic (i.e., negative) peak (Figure 1b), consistent with our previous study (*26*). The endothermic peak represents the unfolding of protofibrils. The magnitude of the exothermic peak became significant as the protein concentration was increased. For the protofibrils at 50 μM β2-m, after cooling from the first run, the second DSC thermogram showed a $C_{p,app}$ trace with an entirely exothermic effect, suggesting the generation of different species or aggregates during the exothermic reaction after the unfolding of protofibrils. Here, the increase in $C_{p,app}$ above 100 °C in the first run is assumed to correspond to the disruption of the newly generated structure. The structure remained partly stable at 120 °C, based on the unsaturated $C_{p,app}$ value at this temperature. This increase in $C_{p,app}$ reminds us of the heat-induced depolymerization of mature fibrils producing the acid-unfolded monomers (see Figure 1 of ref *25*).

In general, it is quite difficult to reproducibly obtain the negative $C_{p,app}$ trace associated with the aggregation of proteins because of its heterogeneous and transient nature in the initial stages (*21*−*24*). To overcome this problem, we examined the effect of heat on larger aggregates of protofibrils produced intentionally by agitation, expecting a species with a negative $C_{p,app}$ trace to be generated more efficiently due to stronger intermolecular interactions. As expected, negative $C_{p,app}$ traces were reproducibly obtained with the aggregated protofibrils.

First, the salt-induced protofibrils in 0.5 M NaCl at pH 2.5 or the acid-unfolded monomers without NaCl at pH 2.5 were agitated by the cylinder in the cell of the isothermal titration calorimeter for 24 h at 37 °C. While we used this cell for convenience, this would not be essential as long as the agitation can be controlled. The agitation resulted in the

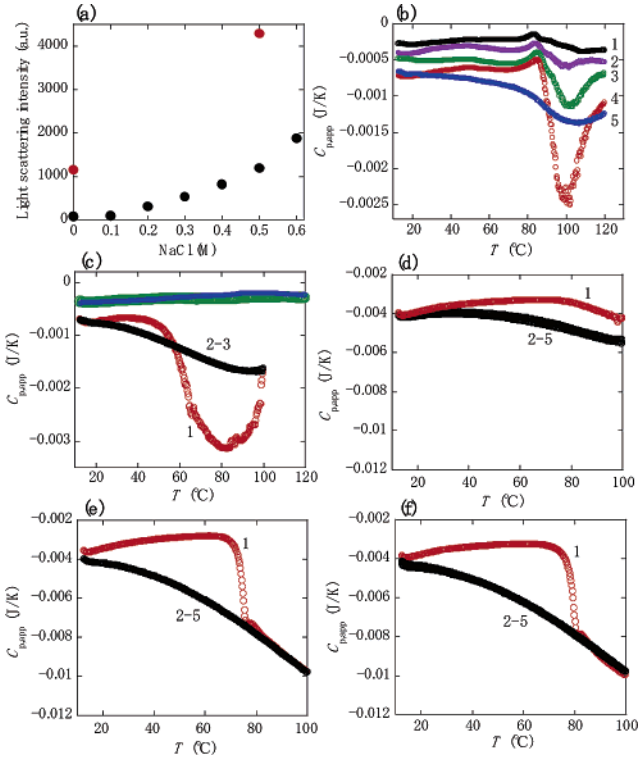

FIGURE 1: Exothermic effects of the aggregated protofibrils of β2-m at pH 2.5. (a) Salt-induced formation of protofibrils. The level of formation of fibrils at various concentrations of NaCl was estimated from the increase in light scattering intensity at 350 nm (●). The red circles correspond to the agitation-treated aggregates produced from the acid-unfolded β2-m at 0 M NaCl and the salt-induced protofibrils at 0.5 M NaCl (see Materials and Methods). The concentration of β2-m was 30 μM. (b) DSC thermograms of the salt-induced protofibrils at 0.5 M NaCl. The protein concentration was varied: (1) 20, (2) 30, (3) 40, (4) 50, and (5) 50 μM (reheating of 4). (c) DSC thermograms of acid-unfolded β2-m (30 μM) at 0 M NaCl and the agitation-treated aggregate solution from the same sample. The green line represents the data for acid-unfolded β2-m, and red and black lines represent the data for the aggregate solution [(1) first run and (2 and 3) second and third runs, respectively]. The blue line represents the second thermogram of the aggregate solution after it was heated to 120 °C and cooled. (d−f) DSC thermograms of an agitation-treated aggregate solution of the salt-induced protofibrils formed at 0.5 M NaCl. The β2-m concentration was varied: (d) 20, (e) 30, and (f) 40 μM. The numbers 1−5 correspond to the number of DSC scans. In all the DSC thermograms, the heating rate was 60 °C/h.

formation of larger aggregates as indicated by the increase in light scattering (red circles in Figure 1a).

Then, DSC thermograms of the agitation-treated samples were measured at 60 °C/h. In the absence of salt, a negative $C_{p,app}$ associated with a sigmoidal transition was observed in the first heating run (Figure 1c). Above 80 °C, the $C_{p,app}$ increased steeply, suggesting the melting of the induced structure. After the sample had cooled from the first run to 100 °C, the subsequent second and third DSC thermograms showed reproducible $C_{p,app}$ traces with an exothermic effect, indicating the generation of different species after the transition in the first run. In contrast, the acid-unfolded form in the absence of NaCl without the agitation treatment exhibited a flat line with a slightly negative $C_{p,app}$ value, indicating that the agitation is important for the generation of species with the exothermic effect. Interestingly, the $C_{p,app}$ values of the second and third DSC thermograms of the agitation-treated sample overlapped with the end point at 100

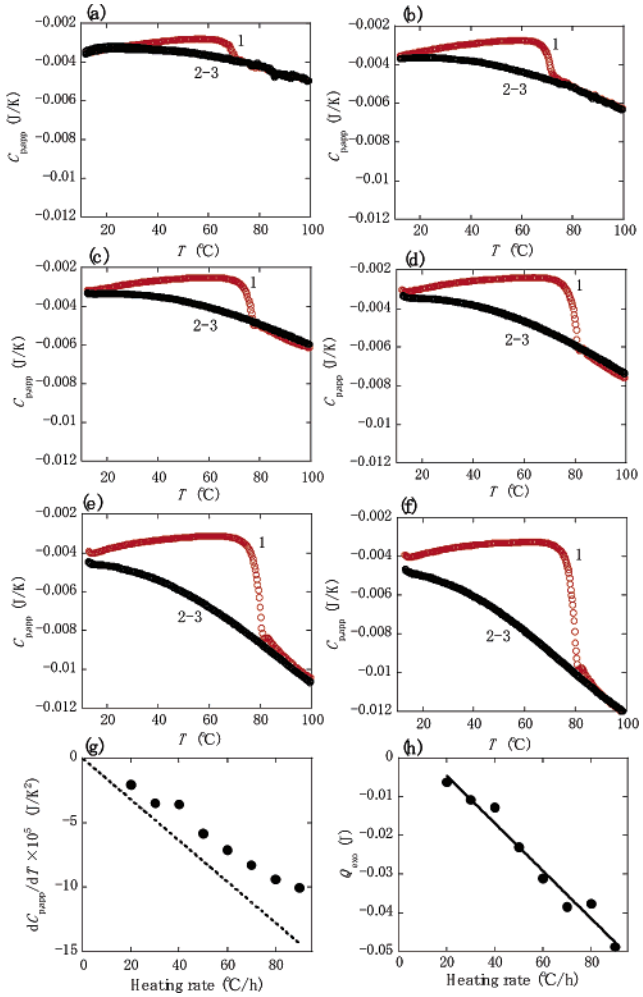

FIGURE 2: Heating rate dependence on the exothermic effect of the agitation-treated aggregate solution of β2-m at pH 2.5. (a−f) Repeated DSC thermograms at the various heating rates: (a) 20, (b) 30, (c) 40, (d) 50, (e) 70, and (f) 90 °C/h. The numbers 1−3 represent the number of DSC scans. The agitation-treated aggregates were produced from the salt-induced protofibrils (30 μM) formed at 0.5 M NaCl. (g) Heating rate dependence of $dC_{p,app}/dT$ values at 60 °C. The $dC_{p,app}/dT$ values were evaluated in the temperature range of 58.5−61.5 °C from the linear slope of the second $C_{p,app}$ trace obtained at various heating rates in panels a−f. The dotted lines represent the corresponding value of well-organized mature amyloid fibrils of β2-m, which were formed by the extension reaction at 37 °C and were taken from ref *26*. (h) Heating rate dependence of Q_{exo} values. The Q_{exo} values were evaluated from the area enclosed by the two $C_{p,app}$ traces of heating runs 1 and 2 as shown in panels a−f. The solid line was linearly fit best to the data.

°C of the $C_{p,app}$ trace in the first run, as was the case with 0.5 M NaCl (see below). Additionally, for this agitation-treated sample, the $C_{p,app}$ value rose further over the temperature above 100 °C and reached that of the monomeric acid-unfolded β2-m at 120 °C (data not shown). The second heating after cooling from 120 °C induced no unique $C_{p,app}$ trace corresponding to that of the acid-unfolded state (Figure 1c), indicating that the heat-induced structure produced by the first scan completely disintegrated with the heating to 120 °C. These results suggest that the partial melting of the induced structure resulted in the intricate DSC thermograms.

Similarly, repeated $C_{p,app}$ traces of the agitation-treated protofibrils in 0.5 M NaCl were recorded at 60 °C/h, an experiment in which the β2-m concentration was varied (20,

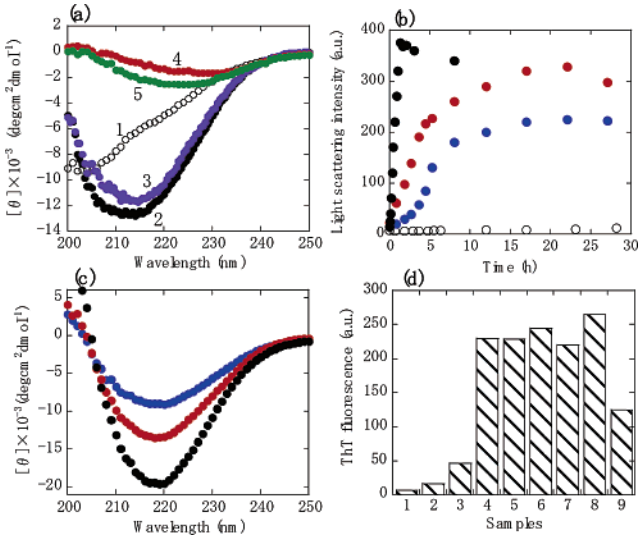

FIGURE 3: Characterization of the species formed after the heat-induced transition of the agitation-treated protofibrils at pH 2.5. (a) Far-UV CD spectra of β2-m in the various states: (1) acid-unfolded state, (2) salt-induced protofibrils formed at 0.5 M NaCl, (3) agitation-treated protofibrils, (4) species formed after the heat-induced transition from the agitation-treated protofibrils, in which the sample was taken out of the DSC cell after heating from 10 to 100 °C at 60 °C/h and cooling, and (5) the same sample as 4, but subjected to four cycles from 20 to 100 °C at 60 °C/h in the thermoelectrically controlled CD cell holder. The protein concentration was 30 μM. (b) Seeding-dependent amyloid fibril growth monitored by measuring light scattering. The solution contained 30 μM β2-m and seed fibrils at 5.0 μg/mL (0.42 μM). Four types of seed fibrils were used: (empty circles) salt-induced protofibrils, (blue circles) agitation-treated protofibrils, (red circles) heat-induced species produced from the agitation-treated protofibrils by heating from 10 to 100 °C at 60 °C/h in the DSC cell, and (black circles) mature β2-m amyloid fibrils. The salt-induced protofibrils were the same as in panel a. The mature β2-m amyloid fibrils were prepared by a seed-dependent extension reaction as described previously (*25*, *26*). The seeds except for the salt-induced protofibrils were fragmented by sonication (*13*). (c) Far-UV CD spectra of the mature amyloid fibrils after the completion of the extension reaction in panel b. Marks are the same as in panel b. (d) Changes in ThT fluorescence intensity associated with the heat-induced transition. The samples numbered 1−3 are the same as those of the same number in panel a. The numbers 4−6 represent the heat-induced species from the agitation-treated protofibrils in panel a, in which each sample was taken from the DSC cell after it had been heated from 10 to 100 °C at 20 (4), 60 (5), and 90 °C/h (6) and cooled, respectively. The numbers 7−9 indicate the fibrils formed by the extension reaction in panel b [7 (blue circles), 8 (red circles), and 9 (black circles)] in which the color marks are the same as in panel b. The samples were diluted with 50 mM sodium citrate buffer at pH 2.5, and the final concentrations of ThT and β2-m were 10 and 6 μM, respectively.

30, 40, and 50 μM). A similar exothermic effect was clearly observed at 30−50 μM β2-m (Figure 1d−f, data not shown for 50 μM). Namely, an abrupt decrease in $C_{p,app}$ occurred at ∼70−80 °C in the first run, followed by a reproducible exothermic thermal response in the subsequent heating runs. In contrast to the thermogram in the absence of NaCl, the intensely negative $C_{p,app}$ value after the transition was retained even above 80 °C and during the subsequent DSC scans. Again, these results indicate that the agitation helps to generate species with a distinct exothermic effect. The screening of a strong electrostatic repulsion between the positively charged β2-m molecules at pH 2.5 by NaCl seems to increase both the starting temperature of the transition and the thermal stability of the species formed by the transition. The absence of a melting transition (i.e., the increase in $C_{p,app}$) in the presence of 0.5 M NaCl is consistent with the increased stability of mature amyloid fibrils in the presence of NaCl (*25*). As will be shown below, this species with the unique exothermic effect is a mature amyloid fibril.

The dependence of this unique $C_{p,app}$ trace on the rate of heating was investigated at 20−90 °C/h with the agitation-treated protofibrils at 30 μM β2-m in 0.5 M NaCl (Figure 2a−f). The repeated $C_{p,app}$ traces revealed a clear transition in the first run, followed by a reproducible exothermic response at all the heating rates that were studied, with the magnitude of the exothermic effect increasing as the heating rate increased. This shows that the thermal response is under kinetic control, precluding the interpretation in terms of equilibrium thermodynamics. The $dC_{p,app}/dT$ values at 60 °C, estimated from the second $C_{p,app}$ trace after the transition, were plotted against the heating rate, characterizing the dependence (Figure 2g). For comparison, the corresponding heating rate dependence of the mature amyloid fibrils taken from our previous paper (*26*) was also presented. The plots show that the two kinetic thermal responses are very similar to each other. The heat (Q_{exo}) needed to induce the kinetic thermal response, i.e., the area enclosed by heating runs 1 and 2, was estimated from the $C_{p,app}$ traces as shown in Figure 2a−f using Origin (Microcal, Inc.) and plotted as a function of the heating rate. The Q_{exo} values were found to be almost linearly dependent on the heating rate, similar to the heating rate-dependent heat flow observed for the mature amyloid fibrils of β2-m and amyloid β peptides (*25*). These results suggest that the protofibrils were converted into mature amyloid fibrils during the first run at all the heating rates that were studied, which was experimentally confirmed below.

Characterization of the Heat-Induced Species. Far-UV CD spectra were recorded to detect the conformational change before and after the heat-induced transition associated with the large decrease in $C_{p,app}$ (Figure 3a). The monomeric β2-m in the absence of salt at pH 2.5 exhibited a somewhat negative ellipticity over the wavelength range of 200−250 nm, characteristic of an acid-unfolded state (*15*). The far-UV CD of the salt-induced protofibrils at 0.5 M NaCl was characterized by a β-sheet spectrum with a minimum at ∼212 nm, consistent with the previous report (*15*). Agitation of the protofibrils inside the cell of the isothermal titration calorimeter did not affect the shape of the spectrum, showing that a significant conformational change was not induced upon the aggregation of protofibrils. This CD spectrum of a β-sheet with a minimum at 212 nm was completely disrupted after the heat-induced transition. Instead, the spectrum exhibited a weak minimum at ∼230 nm, reminiscent of the spectrum often observed when a protein solution contains a notable amount of visible aggregates. Importantly, the repeated heating gradually shifted the minimum to a shorter wavelength, accompanied by an increase in the minimum intensity for the sample subjected to heat-induced transition (Figure 3a), despite the fact that the corresponding $C_{p,app}$ traces were superimposable (Figure 1e). These results imply that the conformational property responsible for the unique thermal response is already created in the specific structure as revealed by CD. Although the sample after the heat-induced transition may contain a significant amount of

β-sheet, the unusual shape of the CD spectrum notably affected by aggregation made it difficult to estimate the exact β-sheet content, as discussed below.

To examine the role of heat-induced species as an amyloid template, seeding experiments with monitoring of light scattering were carried out at pH 2.5 and 37 °C (Figure 3b). For comparison, experiments were also performed with the following species as seeds: salt-induced protofibrils, their agitation-induced aggregates without heat treatment, and mature fibrils prepared in a standard seeding reaction at pH 2.5 (*11*). No significant fibril growth was observed for the salt-induced protofibrils. In the presence of agitation-treated protofibrils, the increase in light scattering was observed with a lag time, resulting in a sigmoidal time course. This suggests that the aggregated protofibrils can act as seeds even if their potential is not high. When the heat-induced species (i.e., species converted by heating from the same aggregated protofibrils) was used as seeds, the extension reaction was further accelerated, eliminating a noticeable lag time, although the reaction was still slower than that with mature fibrils. These results indicate that the heat-induced species acts as an efficient template in the extension reaction.

The maximum intensity in the plateau region of light scattering after the completion of the extension reaction differed among these samples, suggesting a difference in fibril content or morphology (Figure 3b). In fact, the far-UV CD spectra after the extension reaction exhibited a different β-sheet content with a minimum at 219 nm, which is typical for well-organized mature fibrils (Figure 3c). The amyloidogenic propensity of the species formed after the heat-induced transition at various heating rates was assessed by using ThT (Figure 3d). A significantly enhanced fluorescence emission of ThT was observed for these heat-induced species (Figure 3d, columns 4−6). The three types of fibrils formed by the extension reaction also exhibited an intense emission of ThT. The fibrils formed by seeding with the mature fibrils led to a ThT fluorescence lower than those of other fibrils (Figure 3d, columns 7−9), implying that seeds affect the blocking or burial of ThT binding sites of the fibrils extended from them. The results in Figure 3d suggest that the heat-induced form, as well as the fibrils formed by its seeding, already contains a significant amount of organized cross-β-sheet structure, even though the CD spectrum with a small minimum at 230 nm was unusual (Figure 3a). Since the effects of aggregation on the ThT fluorescence and CD spectrum are unknown, we did not perform a quantitative comparison of the various fibrillar species in terms of CD, ThT, or light scattering intensities.

To characterize the morphology of various fibrillar species, the electron micrographs of these samples were examined (Figure 4). The salt-induced protofibrils were thin (2−5 nm in diameter) and curved as previously reported (*15*) (Figure 4a). The protofibrils aggregated via agitation indeed exhibited a mixed morphology of protofibrils and their clusters or aggregates (Figure 4b). Remarkably, the micrographs of the species converted by heating at a rate of 60 °C/h from the same aggregated protofibrils revealed the presence of straight and relatively thick fibrils (10−20 nm in diameter), in which some of them were in a dispersed state (Figure 4c, 1), and others were clusters of relatively short fibrils (Figure 4c, 2). Similarly, the same types of fibrils and cluster states were formed after the heat treatment at the different heating rates of 20 and 90 °C/h (Figure 4d,e). The protofibrils were hardly detected, suggesting that the heat treatment converted most of them into mature fibrils. The fibrils with the same morphology as in Figure 4c−e were reproduced by the

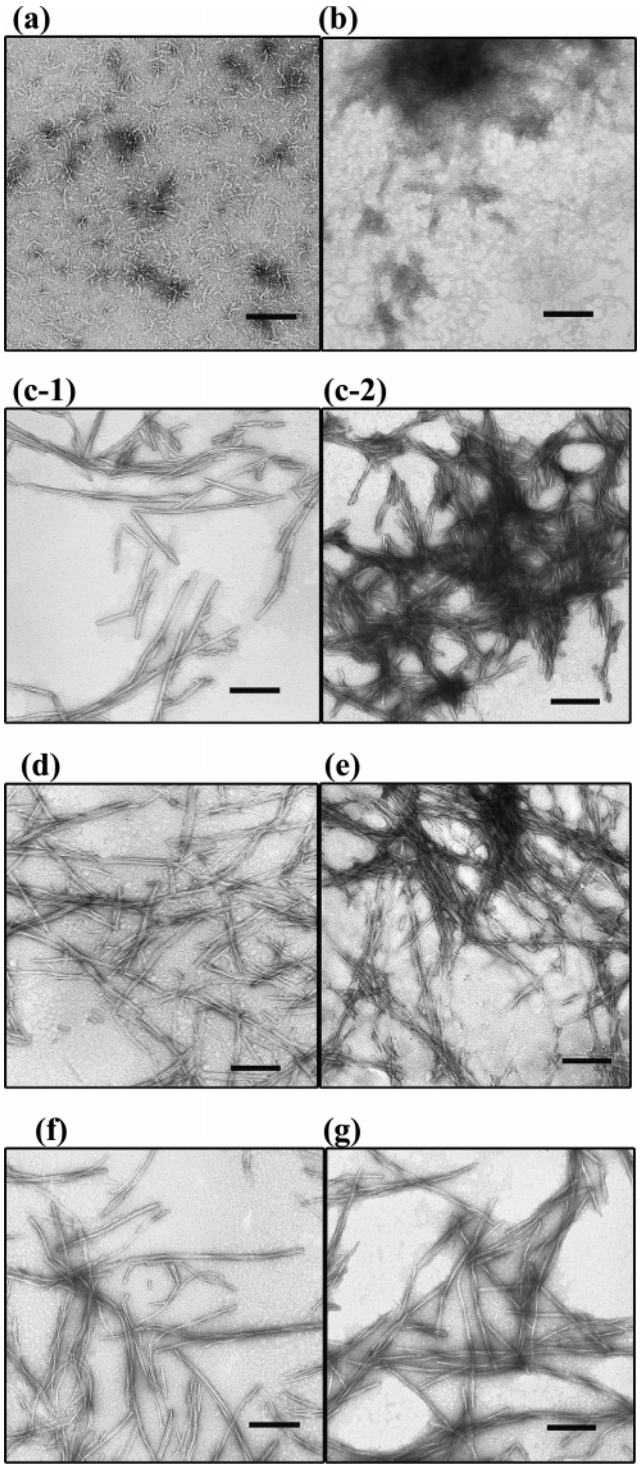

FIGURE 4: Electron micrographs of fibrillar states of β2-m. (a) Salt-induced protofibrils formed at 0.5 M NaCl. (b) Agitation-treated aggregates of the protofibrils in panel a. (c−e) Amyloid fibrils converted from the aggregates in panel b by being heated from 10 to 100 °C and cooled in the DSC cell. The heating rate was varied: (c-1 and c-2) 60, (d) 20, and (e) 90 °C/h. (f) Amyloid fibrils formed by the extension reaction in Figure 3b where the species in panel c was used as the seed. (g) Amyloid fibrils formed by the extension reaction in Figure 3b where the mature amyloid fibrils were used as the seed. The black bar represents 200 nm.

extension reaction, in which the heat-induced species and the mature amyloid fibrils were used as seeds (see panels f and g of Figure 4, respectively). As a result, the observations of morphology by electron microscopy demonstrated that the salt-induced protofibrils in the aggregated state were converted through the heat-induced transition into the well-organized mature amyloid fibrils.

DISCUSSION

Mature Amyloid Formation Triggered by Agitation and Heating. Most strikingly, heating the aggregated protofibrils in 0.5 M NaCl at pH 2.5 transformed them into mature fibrils accompanied by a large decrease in heat capacity. The protofibrils of β2-m in the presence of high concentrations of salts have been considered to be a dead-end product separated from the pathway leading to mature fibrils (*15*, *17*, *18*, *28*). However, since mature fibrils are likely to be made of several thinner protofibrils, salt-induced protofibrils have been studied extensively as a model of "native protofibrils". The present results argue that two fibrillar structures, i.e., mature fibrils and salt-induced protofibrils, can be linked by a certain mechanism, and the change in heat capacity of the protein solution is an important clue for elucidating the link. It is conceivable that the agitation-induced aggregation of protofibrils renders protein molecules susceptible to interactions between adjacent molecules for the promotion of the conformational rearrangement into mature fibrils. Importantly, the aggregation of protofibrils is itself not enough to generate mature fibrils, but in combination with heating, it effectively triggers the conversion, probably because of the increased hydrophobic effect upon heating.

However, it is still not clear whether most of the protofibrils are converted directly into mature fibrils or indirectly through β2-m monomers produced by the depolymerization of protofibrils. Recently, Goldsbury et al. (*29*) suggested that, during the assembly of fibrils from amyloid β peptide, mature fibrils arise from a conformational transition in the protofibrils. Additionally, the observation presented here reflects the fact that agitation (i.e., shaking, rotation, or ultrasonication of the solution) generally promotes the formation of amyloid fibrils, including the case of β2-m, in which an important step is the formation of agitation-induced amorphous aggregates (*28*, *30*, *31*). Thus, although the conditions are different, our results are also interpreted in the context of the aggregation-induced formation of amyloid fibrils, in which the chance of forming the amyloid templates might be enhanced. It is conceivable that the critical templates are formed directly by aggregation and heating of the protofibrils and then subsequent growth proceeds through depolymerized monomers or oligomers.

Considering the importance of agitation that promotes the fibrillation, it would be interesting to address the superiority of the agitation−heating method used in this study to the switched heating−agitation method. As shown in Figure 1b, the salt-induced protofibrils show an endothermic peak at ~85 °C upon heating, corresponding to the unfolding. Although the sample basically returns from the unfolded state to the original protofibrils after cooling, the exothermic reaction becomes notable after the endothermic peak with the increase in protofibril concentration, resulting in the generation of different aggregate species (number 5 in Figure 1b). In the heating−agitation method, agitation of the sample like this could have a strong possibility of converting the sample into mature fibrils. However, as shown in this work, the agitation−heating method has the advantage of being able to reveal the conversion from the agitation-induced protofibrils into the mature fibrils as a sigmoidal transition reflected in the heat capacity of solution.

Heat Capacity Change Associated with Mature Fibril Formation. Another important observation is that the heating rate-dependent kinetic thermal response was observed after the sigmoidal transition of $C_{p,\mathrm{app}}$. It is noteworthy that the starting $C_{p,\mathrm{app}}$ in the DSC thermograms shifted to more negative values following the agitation, particularly for the salt-induced protofibrils (Figure 1d−f), approximately −0.004 J/K at 20 °C, and were almost constant against the heating rates (Figure 2). This indicates that the heat capacity of a protein solution is highly susceptible to the extent of aggregation in terms of the protein−protein and protein−water interactions or the sedimentation of larger aggregates. Hence, the significance of the $C_{p,\mathrm{app}}$ value itself remains unclear. Nevertheless, it is important to note that the kinetic thermal response after the sigmoidal transition of $C_{p,\mathrm{app}}$ showed no notable heating rate dependence at lower temperatures (approximately −0.004 J/K at 20 °C, Figure 2).

The electron micrographs (Figure 4c−e) revealed that the sigmoidal transition of $C_{p,\mathrm{app}}$ corresponds to the conversion of the protofibrils into the well-organized amyloid fibrils, which is also supported by the additional evidence of the enhanced ThT fluorescence (Figure 3d). Thus, it follows that mature fibrils formed after the transition caused a kinetic thermal response. Here, the amount of mature fibril formed by the first DSC scan might not be so great given the shape of the CD spectrum with a minimum peak at ~230 nm (Figure 3a). However, this unusual CD spectrum could arise from the presence of aggregated mature fibrils (Figure 4c, 2). In fact, repeated heating caused the increase in the intensity of the minimum peak in the CD spectrum, suggesting the dispersion of aggregated fibrils and the growth of fibrils (Figure 3a). Therefore, in conjunction with the significantly enhanced ThT fluorescence after the heat-induced transition (Figure 3d, columns 4−6), we consider the amount of β-sheet generated after the transition to be much greater than the estimation from the unusual CD spectrum (Figure 3a).

In the case of the heating of acid-unfolded β2-m in the presence of amyloid seeds, the conversion of 12% of the β2-m monomers into mature amyloid fibrils revealed a similar sigmoidal transition of $C_{p,\mathrm{app}}$, followed by a similar kinetic thermal response (*26*). From these experimental results, it is presumed that a kinetic thermal response is observed when the cross β-sheet content characteristic of well-organized amyloid fibrils reaches a critical level. In fact, the largely negative $C_{p,\mathrm{app}}$ traces overlapped after the transition in the repeated heating runs, despite the probable growth in β-sheet content (Figures 1e and 3a). Furthermore, for the amyloid fibrils converted from agitation-treated protofibrils and the mature fibrils formed by the extension reaction, very similar kinetic thermal responses were found (Figure 2g,h).

Unique DSC Profile and Mature Fibril Structure. In this study, the experiments were mainly conducted in the presence of NaCl at 0.5 M to produce the protofibrils and their aggregates by agitation. Under this condition, the $C_{p,\mathrm{app}}$ traces

of the mature fibrils converted from the aggregated protofibrils did not show a melting transition even at 100 °C (i.e., the increase in $C_{p,\mathrm{app}}$). Our data in the previous paper (*25*) showed that addition of NaCl from 0.1 to 1.0 M into a mature fibril solution of β2-m has a significant effect on the stabilization of fibril structure; the melting point of these fibrils increased upon heating from 75 to >120 °C, in which the unique kinetic thermal response was observed over the wide range of NaCl concentration (~1.5 M) (see Figure 4 of ref *25*). However, an increase in the melting point like this is not generally expected for the native β2-m at neutral pH with the addition of NaCl (0−1.0 M); the melting point increased from approximately 63 to 68 °C (unpublished data). These results imply that the mechanism of stabilization of mature fibrils and native structure of β2-m by salt is considerably different. The difference in residues exposed on the surface, the arrangement of these residues, and the supra-architecture of mature fibrils seem to significantly influence the stabilization of fibrils by salt.

In view of the importance of heating, it would be worth addressing the structural properties of the fibrils converted by the heating at different rates (Figure 2a−f). The electron microscopy and ThT assay revealed that the morphology and the binding ability to ThT were much alike for the fibrils converted at different rates (Figures 3d and 4c−e). These results indicate that the same type of amyloid fibrils is formed uniformly after the transition accompanied by a sigmoidal decrease in $C_{p,\mathrm{app}}$ at the different rates of heating. Then, which structural properties are responsible for the sigmoidal transition leading to the remarkably decreased $C_{p,\mathrm{app}}$ value and for the kinetic thermal response after the transition? Although the exact mechanism underlying these thermal responses remains unclear, the $C_{p,\mathrm{app}}$ data in this study strongly suggest that a structural change to the protein molecule occurs and the property of protein−water interaction varies at the temperature at which the sigmoidal exothermic transition occurs. The properties of the solvent water are integral to the hydration of hydrophobic and polar groups and the formation of hydrogen bonds with the side chains and backbone polar groups (*32*−*35*). Although they play a major role in specifying the basic architecture of both the native fold and amyloid fibrils, the contribution of each factor may differ greatly between the two, resulting in distinct calorimetric properties. As suggested in the previous papers (*25*, *26*), the exothermic effects unique to amyloid fibrils might be attributed to a heating-dependent organization of the amyloid−water network that includes changes in the solvent-accessible surface area of fibrils or in the motion of solvent water molecules trapped in the fibrillar suprastructures (*35*).

Besides the well-organized amyloid fibrils, the formation of flexible and curved fibrils via another assembly route has been reported for other proteins and peptides (*36*−*39*), and such complex kinetic behavior of amyloid assembly was recently discussed by Bader et al. (*39*). The presence of various fibrillar and amorphous aggregates is also true with β2-m. However, the kinetic thermal responses observed for the mature fibrils of β2-m have not been observed for other states, i.e., the native form, amorphous aggregates, or salt-induced protofibrils without agitation. Thus, regardless of the underlying molecular mechanism, the characteristic DSC profile will be an important and useful probe for detecting the formation of amyloid fibrils.

ACKNOWLEDGMENT

Electron micrographs were recorded using a facility in the Research Center for Ultrahigh Voltage Electron Microscopy, Osaka University.

REFERENCES

1. Thirumalai, D., Klimov, D. K., and Dima, R. I. (2003) Emerging ideas on the molecular basis of protein and peptide aggregation, *Curr. Opin. Struct. Biol. 13*, 146−159.
2. Ross, C. A., and Poirier, M. A. (2004) Protein aggregation and neurodegenerative disease, *Nat. Med. 10*, s10−s17.
3. Dobson, C. M. (2006) Protein aggregation and its consequences for human disease, *Protein Pept. Lett. 13*, 219−227.
4. Sunde, M., and Blake, C. (1997) The structure of amyloid fibrils by electron microscopy and X-ray diffraction, *Adv. Protein Chem. 50*, 123−159.
5. Tycko, R. (2004) Progress towards a molecular-level structural understanding of amyloid fibrils, *Curr. Opin. Struct. Biol. 14*, 96−103.
6. Makin, O. S., and Serpell, L. C. (2005) Structures for amyloid fibrils, *FEBS Lett. 272*, 5950−5961.
7. Fändrich, M., and Dobson, C. M. (2002) The behaviour of polyamino acids reveals an inverse side chain effect in amyloid structure formation, *EMBO J. 21*, 5682−5690.
8. Chiti, F., Webster, P., Taddei, N., Clark, A., Stefani, M., Ramponi, G., and Dobson, C. M. (1999) Designing conditions for in vitro formation of amyloid protofilaments and fibrils, *Proc. Natl. Acad. Sci. U.S.A. 96*, 3590−3594.
9. Bjorkman, P. J., Saper, M. A., Samraoui, B., Bennett, W. S., Strominger, J. L., and Wiley, D. C. (1987) Structure of the human class I histocompatibility antigen, HLA-A2, *Nature 329*, 506−512.
10. Yamamoto, S., and Gejyo, F. (2005) Historical background and clinical treatment of dialysis-related amyloidosis, *Biochim. Biophys. Acta 1753*, 4−10.
11. Naiki, H., Hashimoto, N., Suzuki, S., Kimura, H., Nakakuki, K., and Gejyo, F. (1997) Establishment of a kinetic model of dialysis-related amyloid fibril extension in vitro, *Amyloid 4*, 223−232.
12. Ban, T., Hamada, D., Hasegawa, K., Naiki, H., and Goto, Y. (2003) Direct observation of amyloid fibril growth monitored by thioflavin T fluorescence, *J. Biol. Chem. 278*, 16462−16465.
13. Kardos, J., Yamamoto, K., Hasegawa, K., Naiki, H., and Goto, Y. (2004) Direct measurement of the thermodynamic parameters of amyloid formation by isothermal titration calorimetry, *J. Biol. Chem. 279*, 55308−55314.
14. Myers, S. L., Jones, S., Jahn, T. R., Morten, I. J., Tennent, G. A., Hewitt, E. W., and Radford, S. E. (2006) A systematic study of the effect of physiological factors on β_2-microglobulin amyloid formation at neutral pH, *Biochemistry 45*, 2311−2321.
15. Hong, D.-P., Gozu, M., Hasegawa, K., Naiki, H., and Goto, Y. (2002) Conformation of β_2-microglobulin amyloid fibrils analyzed by reduction of the disulfide bond, *J. Biol. Chem. 277*, 21554−21560.
16. Raman, B., Chatani, E., Kihara, M., Ban, T., Sakai, M., Hasegawa, K., Naiki, H., Rao, C. M., and Goto, Y. (2005) Critical balance of electrostatic and hydrophobic interactions is required for β_2-microglobulin amyloid fibril growth and stability, *Biochemistry 44*, 1288−1299.
17. Gosal, W. S., Morten, I. J., Hewitt, E. W., Smith, D. A., Thomson, N. H., and Radford, S. E. (2005) Competing pathways determine fibril morphology in the self-assembly of β_2-microglobulin into amyloid, *J. Mol. Biol. 351*, 850−864.
18. Radford, S. E., Gosal, W. S., and Platt, G. W. (2005) Towards an understanding of the structural molecular mechanism of β_2-microglobulin amyloid formation in vitro, *Biochim. Biophys. Acta 1753*, 51−63.
19. LeVine, H., III (1999) Quantification of β-sheet amyloid fibril structures with thioflavin T, *Methods Enzymol. 309*, 274−284.
20. Uversky, V. N., and Fink, A. L. (2004) Conformational constraints for amyloid fibrillation: The importance of being unfolded, *Biochim. Biophys. Acta 1698*, 131−153.
21. Sanchez-Ruiz, J. M., Lopez-Lacomba, J. L., Cortijo, M., and Mateo, P. L. (1988) Differential scanning calorimetry of the irreversible thermal denaturation of thermolysin, *Biochemistry 27*, 1648−1652.

22. Weijers, M., Barneveld, P. A., Cohen Stuart, M. A., and Visschers, R. W. (2003) Heat-induced denaturation and aggregation of ovalbumin at neutral pH described by irreversible first-order kinetics, *Protein Sci. 12*, 2693−2703.
23. Azuaga, A. I., Dobson, C. M., Mateo, P. L., and Conejero-Lara, F. (2002) Unfolding and aggregation during the thermal denaturation of streptokinase, *Eur. J. Biochem. 269*, 4121−4133.
24. Rezaei, H., Choiset, Y., Eghiaian, F., Treguer, E., Mentre, P., Debey, P., Grosclaude, J., and Haertle, T. (2002) Amyloidogenic unfolding intermediates differentiate sheep prion protein variants, *J. Mol. Biol. 322*, 799−814.
25. Sasahara, K., Naiki, H., and Goto, Y. (2005) Kinetically controlled thermal response of β_2-microglobulin amyloid fibrils, *J. Mol. Biol. 352*, 700−711.
26. Sasahara, K., Naiki, H., and Goto, Y. (2006) Exothermic effects observed upon heating of β_2-microglobulin monomers in the presence of amyloid seeds, *Biochemistry 45*, 8760−8769.
27. Chiba, T., Hagihara, Y., Higurashi, T., Hasegawa, K., Naiki, H., and Goto, Y. (2003) Amyloid fibril formation in the context of full-length protein. Effects of proline mutations on the amyloid fibril formation of β_2-microglobulin, *J. Biol. Chem. 278*, 47016−47024.
28. Kad, N. M., Myers, S. L., Smith, D. P., Smith, D. A., Radford, S. E., and Thomson, N. H. (2003) Hierarchical assembly of β_2-microglobulin amyloid in vitro revealed by atomic force microscopy, *J. Mol. Biol. 330*, 785−797.
29. Goldsbury, C., Frey, P., Olivieri, V., Aebi, U., and Müller, S. A. (2005) Multiple assembly pathways underlie amyloid-β fibril polymorphisms, *J. Mol. Biol. 352*, 282−298.
30. Stathopulos, P. B., Scholz, G. A., Hwang, Y. M., Rumfeldt, J. A., Lepock, J. R., and Meiering, E. M. (2004) Sonication of proteins causes formation of aggregates that resemble amyloid, *Protein Sci. 13*, 3017−3027.
31. Ohhashi, Y., Kihara, M., Naiki, H., and Goto, Y. (2005) Ultrasonication-induced amyloid fibril formation of β_2-microglobulin, *J. Biol. Chem. 280*, 32843−32848.
32. Dill, K. A. (1990) Dominant forces in protein folding, *Biochemisrtry 29*, 7133−7155.
33. Perutz, M. F., Finch, J. T., Berriman, J., and Lesk, A. (2002) Amyloid fibers are water-filled nanotubes, *Proc. Natl. Acad. Sci. U.S.A. 99*, 5591−5595.
34. Cordeiro, Y., Kraineva, J., Ravindra, R., Lima, L. M., Gomes, M. P. B., Foguel, D., Winter, R., and Silva, J. L. (2004) Hydration and packing effects on prion folding and β-sheet conversion. High pressure spectroscopy and pressure perturbation calorimetry studies, *J. Biol. Chem. 279*, 32354−32359.
35. Cooper, A. (2005) Heat capacity effects in protein folding and ligand binding: A re-evaluation of the role of water in biomolecular thermodynamics, *Biophys. Chem. 115*, 89−97.
36. Modler, A. J., Gast, K., Lutsch, G., and Damaschun, G. (2003) Assembly of amyloid protofibrils via critical oligomers: A novel pathway of amyloid formation, *J. Mol. Biol. 325*, 135−148.
37. Carrotta, R., Manno, M., Bulone, D., Martorana, V., and San, Biagio, P. L. (2005) Protofibril formation of amyloid β-protein at low pH via a non-cooperative elongation mechanism, *J. Biol. Chem. 280*, 30001−30008.
38. Hurshman, A. R., White, J. T., Powers, E. T., and Kelly, J. W. (2004) Transthyretin aggregation under partially denaturing conditions is a downhill polymerization, *Biochemistry 43*, 7365−7381.
39. Bader, R., Bamford, R., Zurdo, J., Luisi, B. F., and Dobson, C. M. (2006) Probing the mechanism of amyloidogenesis through a tandem repeat of the PI3-SH3 domain suggests a generic model for protein aggregation and fibril formation, *J. Mol. Biol. 356*, 189−208.

BI602403V